International Journal of Heat and Mass Transfer 95 (2016) 35–44

Contents lists available at ScienceDirect

International Journal of Heat and Mass Transfer

journal homepage: www.elsevier.com/locate/ijhmt

A moving boundary model for two-phase flow heat exchanger incorporated with relative velocities between boundaries and fluid

Daijin Li *, Kai Luo, Jianjun Dang

School of Marine Science and Technology, Northwestern Polytechnical University, Xi'an, China

ARTICLE INFO

Article history:
Received 10 September 2015
Received in revised form 27 November 2015
Accepted 28 November 2015

Keywords:
Moving boundary
Two-phase flow
Heat exchanger
Relative velocity

ABSTRACT

Moving Boundary (MB) dynamic model is an appealing approach for investigation of advanced control schemes for two-phase flow heat exchanger. For the confusion of relative velocities between boundaries and fluid existing in the previous MB model, this paper presents a modified moving boundary model. The dynamic model incorporated with the relative velocities is derived from physical principles of mass and energy conservation. And the model is then implemented in a novel underwater HYDROX system to predict cyclic performance. The simulation results from discretized model using MATLAB language show that the oscillations which is known as "*Chattering*" have been suppressed.

1. Introduction

Current heat exchanger (evaporator or condenser) system models are more appropriate for advanced control strategies. Bendapudi and Braun [1] discussed such modeling approaches including both finite volume model and Moving Boundary (MB) model. MB model has been proved much faster by Grald and MacArthur [2], which makes it to be the first choice for control system design [3].

The idea of MB model is to dynamically track the length of different regions in heat exchanger. And then, mass and energy conservation equations are formulated for each Control Volumes (CVs) with variable boundaries. A simple geometry for MB in an evaporator can be seen in Fig. 1.

Several works have described MB dynamic models. Adams et al. [4] pioneered MB models. Ray and Bowman [5] developed a nonlinear model based on the work of Adams. They described a three-region model with time-varying phase boundaries by a set of nonlinear differential and algebraic equations derived from the fundamental equations of conservation of mass, momentum, and energy. Extensions of this work for solar applications are presented in [6,7]. Dhar and Soedel [8] employed a simplified heat exchanger model in which spatial dependency was ignored. Mckinley and Alleyne [9], Mancini [10], Rasmussen [11] and Bonilla et al. [12–14] have presented the remarkable MB model reviews for two-phase flows.

He et al. [15,16] was the first to suggest the use of MB models for multi-input multi-output (MIMO) control design. He presented linearized two-region MB models for the evaporator and condenser with adequate validation. Wei et al. [17] presented MB model approach, separately for refrigeration systems and organic Rankine cycles, extending the work of He et al. [15,16].

Using first principles of mass and energy conservation, along with three separate MB formulations, Jensen [18], Jensen and Tummescheit [19] have presented a general moving boundary model for the conceivable cases of flow, including equations governing radiative, conductive and convective losses. Yebra et al. [20] extended the MB formulation from [15] including the momentum balance equation discretized in CV by the finite volume method in order to account for pressure drop. Li and Alleyne [21] developed a switching evaporator model, extending the condenser model previously developed in [9]. Also, experimental validation was presented by considering two test cases. Gräber et al. [22] derived their MB models in an elegant way from first principles, and proposed a validation procedure based on infrared thermography. Cecchinato and Mancini [23] presented a generalized intrinsically mass conservative evaporator model based on the MB approach. Zapata et al. [24] introduced a dynamic model of a once-through-to-superheat solar steam receiver for electricity generation following the approach presented by Mckinley and Alleyne [9] for refrigeration systems and Wei et al. [17] for Organic Rankine cycles.

An essential aspect of the MB formulation is pressure drop throughout the heat exchanger. Most researchers above assumed the pressure drop in the heat exchanger to have a negligible effect

* Corresponding author.
E-mail address: lidaijin@nwpu.edu.cn (D. Li).

http://dx.doi.org/10.1016/j.ijheatmasstransfer.2015.11.095
0017-9310/

Nomenclature

A	area (m^2)
ρ	density (kg/m^3)
D	diameter (m)
h	enthalpy (J/kg)
q	heat flux per unit length (W/m)
Q	heat (J)
L	length (m)
B_{nz}	nozzle pressure ratio
Nu	Nusselt number
S	perimeter (m)
k	ratio of specific heat
c	specific heat capacity (J/(kg K))
T	temperature (K)
λ	thermal conductivity (W/m K)
v	velocity (m/s)
V	capacity (m^3)
ε	degree of partial admission
η	dynamic viscosity (Pa s)
R_g	gas constant (J/(mol K))
α	heat transfer coefficient (J/(kg m))
v	kinematic viscosity (m^2/s)
m	mass (kg)
α_{nz}	nozzle angle (rad)
Pr	Prandtl number
P	pressure (Pa)
Re	Reynolds number
u	special internal energy (J/kg)
t	time (s)
u_{trb}	turbine linear velocity (m/s)
P_u	wheel power (W)

Subscripts

amb	ambient
cmb	combustor
s	design condition
g	gas phase
i	inner wall
l	liquid phase
o	outer wall
bo	outlet boundary
rw	reagent water
sa	saturation
trb	turbine
av	average
cnd	condenser
evp	evaporator
in	inlet
bi	inlet boundary
nz	nozzle
out	outlet
rdu	reactor
wall	reactor wall
w	tube wall
e	two-phase

on the dynamic response and they calculate thermodynamic properties from the predicted pressure. The exception are Adams et al. [4], Ray and Bowman [5], Yebra et al. [20] and Tian et al. [25,26], where static pressure drop was included. But the lumped thermodynamic properties were still evaluated at isobaric conditions. Also, all researchers above neglected any changes in kinetic energy.

This article uses first principles of mass and energy conservation to produce a modified MB formulation. Differences between this model and previous work are: an explicit inclusion of relative velocities between fluid and boundaries and consideration of pressure loss and kinetic energy. The effects of including these modifications relative to past models are discussed, and this model is shown to be suitable for the development of advanced control algorithms.

2. Previous models

According to the literature [12–20], the general governing equations for the time-dependent equations for conservation laws, applying the nomenclature in Fig. 2, is presented as Eqs. (1) and (2).

Mass balance:

$$A\frac{d}{dt}\int_{z_{in}}^{z_{out}}\rho dz+\rho_{in}A\frac{dz_{in}}{dt}-\rho_{out}A\frac{dz_{out}}{dt}=\dot{m}_{in}-\dot{m}_{out} \tag{1}$$

Energy balance:

$$A\frac{d}{dt}\int_{z_{in}}^{z_{out}}\rho h dz-AL\frac{dp}{dt}+A\rho_{in}h_{in}\frac{dz_{in}}{dt}-A\rho_{out}h_{out}\frac{dz_{out}}{dt}=\dot{m}_{in}h_{in}-\dot{m}_{out}h_{out}+qL \tag{2}$$

where, z_{in} and z_{out} are the locations of the inlet and outlet boundaries; dz_{in}/dt and dz_{out}/dt are the velocities of the boundaries. The "Inlet" and "Outlet" refer to the case of an evaporator and are switched in the case of a condenser.

In the mass balance of Eq. (1), the first term on the left hand side describes the rate of mass change in the CV caused by density change. The second and third terms describe the mass change in the CV due to changes in boundary positions. The two terms on the right hand side are the mass flows through the inlet and outlet boundaries.

In the energy balance of Eq. (2), the first term on the left hand side is the change rate of enthalpy in the CV, the second term is a consequence of using enthalpy and not internal energy in the first term. The third and fourth terms account for the change of enthalpy due to changes in boundary locations. The two first terms on the right hand side are the convective enthalpy through the boundaries, and the last term is the heat flow from the tube wall.

The mass balance shown in Eq. (1), can be physically interpreted that the changes of mass flow rate equal to the sum of

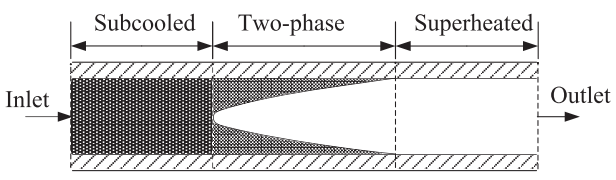

Fig. 1. Schematic of MB for an evaporator.

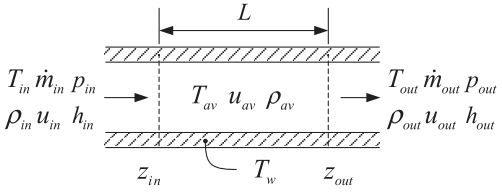

Fig. 2. Schematic of a CV.

changes of mass flow rate caused by density variations and changes of mass flow rate caused by the movement of the boundaries. However, these balance equations are flawed because the fluid velocities relative to the boundaries are not included in the conservation law. Instead, the velocities of the boundaries and fluid velocities are convolved. The aim of the current paper is to modify the governing equations of MB model.

3. Modified MB model

3.1. Governing equations in a CV

In order to get a low order model that still reflects the essential dynamics in a mathematically tractable form, a number of assumptions are made:

- Cylindrical geometry with a constant cross-sectional area.
- Spatial changes in each of the three regions are described by averaged properties using one-dimensional equations.
- Gravitational forces are negligible.
- Two-phase flow is in thermodynamic equilibrium.

For the one-dimensional CV in Fig. 2, the existing relations are shown as:

$$\begin{cases} \frac{dz_{out}}{dt} = v_{bo} \\ \frac{dz_{in}}{dt} = v_{bi} \\ \frac{dL}{dt} = v_{bo} - v_{bi} \end{cases} \tag{3}$$

$$\begin{cases} v_{in} = v_{bi} + v_{ri} \\ v_{out} = v_{bo} + v_{ro} \end{cases} \tag{4}$$

$$\begin{cases} \dot{m}_{in} = A\left(v_{in} - \frac{dz_{in}}{dt}\right)\rho_{in} \\ \dot{m}_{out} = A\left(v_{out} - \frac{dz_{out}}{dt}\right)\rho_{out} \end{cases} \tag{5}$$

where, v_{bi} and v_{bo} are absolute velocities of inlet and outlet boundaries, respectively. v_{in} and v_{out} are absolute velocities of fluid at inlet and outlet, respectively. v_{ri} and v_{ro} are fluid velocities relative to the boundaries at inlet and outlet respectively. Consideration of this relative velocities is the main different between proposed model and previous work.

Mass balance:

$$\dot{m}_{in} - \dot{m}_{out} = A\frac{d}{dt}\int_{z_{in}}^{z_{out}} \rho dz \tag{6}$$

Leibnitz's Rule has been applied [18]. Leibniz's rule for differentiation of integrals with time varying limits reads:

$$\frac{d}{dt}\int_{z_{in}}^{z_{out}} f(z,t)dz = f(z_{out},t)\frac{dz_{out}}{dt} - f(z_{in},t)\frac{dz_{in}}{dt} + \int_{z_{in}}^{z_{out}} \frac{\partial f(z,t)}{\partial t}dz \tag{7}$$

So,

$$\begin{aligned} &\dot{m}_{in} - \dot{m}_{out} = A\tfrac{d}{dt}\textstyle\int_{z_{in}}^{z_{out}} \rho dz \\ &= A\left(\rho_{out}\tfrac{dz_{out}}{dt} - \rho_{in}\tfrac{dz_{in}}{dt} + \textstyle\int_{z_{in}}^{z_{out}} \tfrac{d\rho}{dt}dz\right) \\ &= A\left(\rho_{out}\tfrac{dz_{out}}{dt} - \rho_{in}\tfrac{dz_{in}}{dt} + L\tfrac{d\rho_{av}}{dt}\right) \end{aligned} \tag{8}$$

Energy balance:

$$qL = \frac{d}{dt}\int_0^L A\rho\left(u + \frac{v^2}{2}\right)dz + Ap_{out}(v_{bo} + v_{ro}) - Ap_{in}(v_{bi} + v_{ri}) \tag{9}$$

In Eq. (9), the term on the left hand side represents the heat from the tube wall convected into the fluid. The first term on the right hand side describes the change rate of stagnation energy in the CV, which contains the internal energy and the kinetic energy. The last two terms on the right hand side are the power flows through the boundaries.

The heat flux is modeled using a heat transfer coefficient:

$$q = \alpha(T_w - T_{av})S \tag{10}$$

In single phase region:

$$T_w - T_{av} = \frac{T_{out} - T_{in}}{\ln\left(\frac{T_w - T_{in}}{T_w - T_{out}}\right)} \tag{11}$$

In the two-phase region, the average temperature is calculated as the saturation temperature.

$$T_{av} = T_{sa} \tag{12}$$

Leibnitz's Rule can be applied to the energy balance in Eq. (9),

$$\begin{aligned} qL \doteq A\int_0^L \frac{d(\rho u)}{dt}dz + A\rho_{out}u_{out}(v_{bo} + v_{ro}) - A\rho_{in}u_{in}(v_{bi} + v_{ri}) \\ + Ap_{out}(v_{bo} + v_{ro}) - Ap_{in}(v_{bi} + v_{ri}) \end{aligned} \tag{13}$$

That is,

$$\begin{aligned} qL = A\int_0^L \frac{d(\rho u)}{dt}dz + A\rho_{out}\left(u_{out} + \frac{p_{out}}{\rho_{out}}\right)(v_{bo} + v_{ro}) \\ - A\rho_{in}\left(u_{in} + \frac{p_{in}}{\rho_{in}}\right)(v_{bi} + v_{ri}) \end{aligned} \tag{14}$$

With specific enthalpy, the equation above is expressed as:

$$A\rho_{in}h_{in}(v_{bi} + v_{ri}) - A\rho_{out}h_{out}(v_{bo} + v_{ro}) + qL = AL\frac{d(u_{av}\rho_{av})}{dt} \tag{15}$$

Inserting Eqs. (4) and (5) into the energy balance Eq. (15) yields:

$$\begin{aligned} AL\frac{d(u_{av}\rho_{av})}{dt} + A\rho_{out}h_{out}\frac{dL}{dt} + h_{out}\dot{m}_{out} \\ = h_{in}\dot{m}_{in} + qL + A(\rho_{in}h_{in} - \rho_{out}h_{out})v_{bi} \end{aligned} \tag{16}$$

For the above, Eqs. (8) and (16) are modified forms of the general MB governing equations in Refs. [12–20].

3.2. Boundary conditions

In a system model, the boundary conditions are usually calculated in adjacent models and may be considered as known boundary conditions. Taking evaporators as an example, the design input and output variables are shown in Fig. 3. Boundary conditions are analyzed as described below. For condensers, obtaining boundary conditions is similar.

3.2.1. Subcooled region

For evaporators, the average density and average specific internal energy in the subcooled region is approximated as the arithmetic average of the input and output parameters.

$$\rho_{l,av} = \frac{\rho_{l,in} + \rho_{l,sa}}{2} \tag{17}$$

$$u_{l,av} = \frac{u_{l,in} + u_{l,sa}}{2} \tag{18}$$

According to Eqs. (8) and (16), the governing equations in the subcooled region can be written as:

$$A\rho_{l,av}\frac{dL_l}{dt} + \dot{m}_{l,out} = \dot{m}_{l,in} \tag{19}$$

$$A\rho_{l,sa}h_{l,sa}\frac{dL_l}{dt} + h_{l,sa}\dot{m}_{l,out} = h_{l,in}\dot{m}_{l,in} + q_lL_l \tag{20}$$

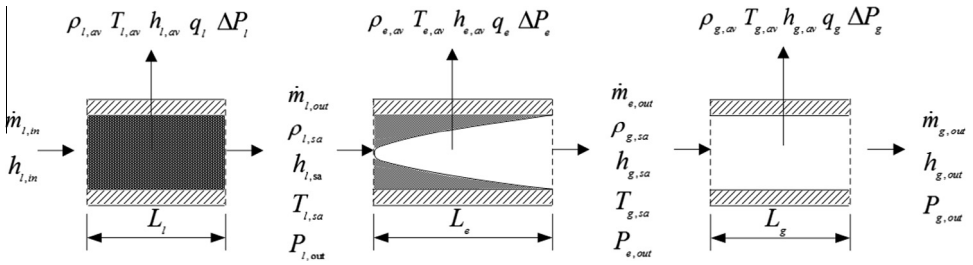

Fig. 3. Design input and output variables.

That is,

$$\dot{m}_{l,out} = \dot{m}_{l,in} - A\rho_{l,av}\frac{dL_l}{dt} \tag{21}$$

$$\frac{dL_l}{dt} = \frac{(h_{l,in} - h_{l,sa})\dot{m}_{l,in} + q_l L_l}{A(\rho_{l,sa} - \rho_{l,av})h_{l,sa}} \tag{22}$$

Heat flux per unit length is written as:

$$q_l = \alpha_l(T_{amb} - T_{l,av})S \tag{23}$$

The heat transfer coefficient α_l is the overall heat transfer coefficient given by:

$$\frac{1}{\alpha_l} = \frac{1}{\alpha_{l,i}} + \frac{1}{\alpha_{l,o}} \tag{24}$$

The heat transfer coefficient for single-phase turbulent flow in a circular tube can be calculated using Gnielinski equation [27].

$$Nu_l = \frac{(f_l/8)(Re_l - 1000)Pr_l}{1 + 12.7(f_l/8)^{1/2}\left(Pr_l^{2/3} - 1\right)}\left[1 + \left(\frac{D_{evp}}{L_l}\right)^{2/3}\right]a_l \tag{25}$$

The Darcy friction coefficient for smooth pipes is calculated using Filonenko's equation [28].

$$f_l = (1.82\ln(Re_l) - 1.64)^{-2} \tag{26}$$

Here, the equations are valid for $2300 < Re_l < 10^6$ and $0.6 < Pr_l < 10^5$ assuming uniform heat flux and temperature. a_l denotes correction coefficient. The Nusselt, Prandtl and Reynolds numbers are defined as:

$$Nu_l = \alpha_{l,i}\frac{D_{evp}}{\lambda_l} \quad Pr_l = \frac{v_l c_P}{\lambda_l} \quad Re_l = \frac{v_l D_{evp}}{v_l} \tag{27}$$

Here, c_P denotes specific isobaric heat capacity.

Average temperature in the subcooled region is expressed in the form of the logarithmic mean temperature difference.

$$T_{l,av} = T_{amb} - \frac{T_{l,sa} - T_{l,in}}{\ln\left(\frac{T_{amb} - T_{l,in}}{T_{amb} - T_{l,sa}}\right)} \tag{28}$$

Pressure loss in subcooled region is calculated as:

$$\Delta p_l = f_l\frac{L_l}{D_{evp}}\frac{\rho_l v_l^2}{2} \tag{29}$$

3.2.2. Two-phase region

According to Eqs. (8) and (16), the governing equations of two-phase region in evaporators is:

$$\dot{m}_{e,out} = \dot{m}_{l,out} - A\rho_{e,av}\frac{dL_e}{dt} \tag{30}$$

$$A\rho_{g,sa}h_{g,sa}\frac{dL_e}{dt} + h_{g,sa}\dot{m}_{e,out} = h_{l,sa}\dot{m}_{l,out} + q_e L_e + A(\rho_{l,sa}h_{l,sa} - \rho_{g,sa}h_{g,sa})\frac{dL_l}{dt} \tag{31}$$

With heat flux per unit length:

$$q_e = \alpha_e(T_{amb} - T_{sa})S \tag{32}$$

The heat transfer coefficient is the overall heat transfer coefficient given by $1/\alpha_e = 1/\alpha_{e,i} + 1/\alpha_{e,o}$. The two-phase flow boiling heat transfer coefficient $\alpha_{e,i}$ can be given by [29]:

$$\frac{\alpha_{e,i}}{\alpha_{l,sa}} = C_1 Co^{C_2} + C_3 Bo^{C_4} \tag{33}$$

In which, $C_1 \sim C_4$ are constants referred in [29]. *Co* is convection number. *Bo* is boiling number.

$$Co = \left(\frac{1 - x_e}{x_e}\right)^{0.8}\left(\frac{\rho_{g,sa}}{\rho_{l,sa}}\right)^{0.5} \quad Bo = \frac{A_{evp}q_e}{\dot{m}_e\Upsilon} \tag{34}$$

Here, x_e is dryness fraction. Υ is latent heat of vaporization. $\alpha_{l,sa}$ can be calculate using Dittus–Boelter equation [30].

$$\alpha_{l,sa} = 0.023Re_{l,sa}^{0.8}Pr_{l,sa}^{0.4}\frac{\lambda_{l,sa}}{D_{evp}} \tag{35}$$

Here, Prandtl, Reynolds numbers are defined as:

$$Fr_{l,sa} = \frac{(\dot{m}_e/A_{evp})^2}{\rho_{l,sa}^2 g D_{evp}} \quad Re_{l,sa} = \frac{(\dot{m}_e/A_{evp})D_{evp}(1 - x_e)}{\eta_{l,sa}} \tag{36}$$

And, the average density:

$$\rho_{e,av} = \gamma_{e,av}\rho_{g,sa} + (1 - \gamma_{e,av})\rho_{l,sa} \tag{37}$$

The void fraction $\gamma_{e,av}$ is:

$$\gamma_{e,av} = \frac{1 - \mu[1 - \ln(\mu)]}{(1 - \mu)^2} \tag{38}$$

The ratio of average phase velocities, called slip ratio [18], is defined as:

$$\mu = \left(\frac{\rho_{g,sa}}{\rho_{l,sa}}\right)^{2/3} \tag{39}$$

Pressure loss in two-phase region is then calculated as:

$$\Delta p_e = f_e\frac{L_e}{D_{evp}}\frac{\rho_{e,av}v_e^2}{2} \tag{40}$$

The friction coefficient in two-phase region is:

$$f_e = (1.82\ln Re_e - 1.64)^{-2} \tag{41}$$

$$Re_e = \frac{\dot{m}_e}{A_{evp}}\frac{D_{evp}}{\eta_e} \tag{42}$$

3.2.3. Superheated region

The averaged properties in the superheated region are calculated in the same way as in the subcooled region.

$$\rho_{g,av} = \frac{\rho_{g,sa} + \rho_{g,out}}{2} \tag{43}$$

According to Eqs. (8) and (16), the balance equations in the superheated region are as follows:

$$A\frac{L_g}{2}\left(\frac{d\rho_{g,sa}}{dp}\frac{dp}{dt}+\frac{\partial\rho_{g,out}}{\partial p}\frac{dp}{dt}+\frac{\partial\rho_{g,out}}{\partial T_{g,out}}\frac{dT_{g,out}}{dt}\right)+A\rho_{g,av}\frac{dL_g}{dt}+\dot{m}_{g,out}=\dot{m}_{e,out} \tag{44}$$

$$AL_g\frac{d(u_{g,av}\rho_{g,av})}{dt}+A\rho_{g,out}h_{g,out}\frac{dL_g}{dt}+h_{g,out}\dot{m}_{g,out}=A(\rho_{g,sa}h_{g,sa}-\rho_{g,out}h_{g,out})\frac{d(L_l+L_e)}{dt}+h_{g,sa}\dot{m}_{e,out}+q_gL_g \tag{45}$$

The geometric relation for the superheated region is:

$$\frac{d(L_l+L_e)}{dt}=\frac{d(L-L_g)}{dt}=-\frac{dL_g}{dt} \tag{46}$$

Inserting Eq. (43) into Eq. (40) yields:

$$AL_g\frac{d(u_{g,av}\rho_{g,av})}{dt}+h_{g,out}\dot{m}_{g,out}=h_{g,sa}\dot{m}_{e,out}+q_gL_g-A\rho_{g,sa}h_{g,sa}\frac{dL_g}{dt} \tag{47}$$

where,

$$\frac{d(u_{g,av}\rho_{g,av})}{dt}=u_{g,av}\frac{d(\rho_{g,sa}+\rho_{g,out})}{2dt}+\rho_{g,av}\frac{d(u_{g,sa}+u_{g,out})}{2dt}\doteq\frac{1}{2}\left(u_{g,av}\frac{\partial\rho_{g,out}}{\partial T_{g,out}}+\rho_{g,av}c_{v,g,out}\right)\frac{dT_{g,out}}{dt} \tag{48}$$

In which, $c_{v,g,out}$ is the specific heat capacity of constant volume.

Inserting Eq. (45) into Eq. (44), the energy balance equation is:

$$A\frac{L_g}{2}\left(u_{g,av}\frac{\partial\rho_{g,out}}{\partial T_{g,out}}+\rho_{g,av}c_{v,g,out}\right)\frac{dT_{g,out}}{dt}+h_{g,out}\dot{m}_{g,out}=h_{g,sa}\dot{m}_{e,out}+q_gL_g-A\rho_{g,sa}h_{g,sa}\frac{dL_g}{dt} \tag{49}$$

Heat flux per unit length is again:

$$q_g=\alpha_g(T_{amb}-T_{g,av})S \tag{50}$$

Average temperature in the subcooled region can also be expressed in the form of the logarithmic mean temperature difference.

$$T_{g,av}=T_{amb}-\frac{T_{g,out}-T_{g,sa}}{\ln\left(\frac{T_{amb}-T_{g,sa}}{T_{amb}-T_{g,out}}\right)} \tag{51}$$

Pressure loss in the superheated region can be calculated as:

$$\Delta p_g=f_g\frac{L_g}{D_{evp}}\frac{\rho_{g,av}v_g^2}{2} \tag{52}$$

The friction coefficient in superheated region is the same as subcooled region.

4. Structure description

The system considered in this paper is characterized by a novel underwater HYDROX system for Unmanned Underwater Vehicles (UUVs), containing a combustor, in which heat from combustion of fuel (H_2) and oxidizer (O_2) is used to heat and evaporate water. The high-temperature, high-pressure steam drives a micro turbine, and the low-pressure turbine exhaust is condensed in longitudinal passages near the outer surface of the structural hull of the UUV. The liquid water is collected in a receiver and pumped back to the system. The structure provides several important advantages. Since the cycle is closed, the UUV's operating performance is independent of depth and there is no external exhaust.

Part of the liquid water from pump (m_1) comes into the reactor, which is a hydrogen generator. And most of this liquid plays the role of reagent in the reactor. The other part (m_2) absorbs heat from the chemical reaction in the reactor via the evaporator coil around its surface. The remaining part (m_3) is fed to the combustor as cooling water. A simplified schematic of the system is illustrated in Fig. 4.

In reactor, an active metal such as aluminum can be used to produce hydrogen through the following exothermic chemical reaction.

$$2Al+3H_2O\rightarrow Al_2O_3+3H_2+Q \tag{53}$$

In combustor, hydrogen from the reactor and oxidizer produce a combustion reaction. Also, superheated vapor from the evaporator, and cooling water from the pump (m_3) can be used to increase the working medium. The steam-gas can be made through the following stoichiometric equation:

$$2H_2+O_2\rightarrow 2H_2O+Q_C \tag{54}$$

According to the system above, water from the pump enters the evaporator in liquid phase and exits as either superheated vapor or a mixture of vapor and steam with a small quality. Conversely, the condenser is characterized by entering superheated vapor and leaving saturated liquid. So, both the evaporator and condenser can be described as composed by three zones characterized by subcooled region, two-phase region and superheated region. For each region, appropriate one-dimensional governing equations can be derived through the modified MB approach presented.

In order to evaluate the thermodynamic performance, the mathematical models for reactor, turbine and combustor are derived as follows.

4.1. Reactor

In the reactor, the net heat power can be written as:

$$\dot{Q}_{rdu}=\dot{Q}+\dot{Q}_{Al}+\dot{Q}_{H_2O}-\dot{Q}_{H_2}-\dot{Q}_{Al_2O_3}-\dot{Q}_{icw} \tag{55}$$

where, Q_{rdu} is net heat from the reactor. Q_{Al} is heat carried into reactor by original metal aluminum. Q_{H_2O} is heat carried into reactor by original fluid water. Q_{H_2} is heat absorbed by the product of hydrogen. $Q_{Al_2O_3}$ is heat absorbed by the product of Al_2O_3. And, Q_{icw} is heat absorbed by the rest water of the chemical reaction.

Energy balance of the reactor can be written as:

$$\dot{Q}_{rdu}-\dot{Q}_{evp}=(m_{wall}c_{wall}+m_{Al}c_{Al}+m_{Al_2O_3}c_{Al_2O_3})\frac{dT_{rdu}}{dt} \tag{56}$$

where, $\dot{Q}_{evp}$ is heat absorbed by evaporator. m_{wall} is mass of reactor wall. m_{Al} is mass of the residual metal aluminum. $m_{Al_2O_3}$ is mass of Al_2O_3 .

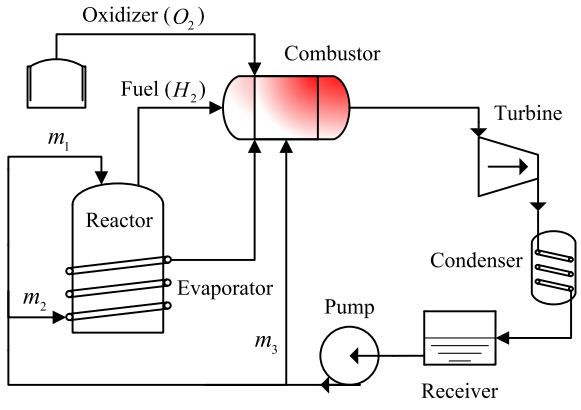

Fig. 4. Schematic diagram of the steam power cycle.

And also,

$$\dot{Q}_{evp} = \dot{Q}_{evp,l} + \dot{Q}_{evp,e} + \dot{Q}_{evp,g} \tag{57}$$

where,

$$\dot{Q}_{evp,l} = q_{evp,l}\pi D_{evp} L_{evp,l} \tag{58}$$

$$\dot{Q}_{evp,e} = q_{evp,e}\pi D_{evp} L_{evp,e} \tag{59}$$

$$\dot{Q}_{evp,g} = q_{evp,g}\pi D_{evp} L_{evp,g} \tag{60}$$

Heat power of the reactor can be written as:

$$\dot{Q}_{rdu} = \frac{1000 Q_{rdu}}{M_{H_2O}} \dot{m}_{rdu,rw} \tag{61}$$

Here, $m_{rdu,rw}$ is mass of reagent water in the reactor. M_{H_2O} is molar mass of water.

According to the chemical equation, mass balance of the reactor is:

$$\dot{m}_{H_2} = \frac{\dot{m}_{rdu,rw}}{9} \tag{62}$$

4.2. Combustor

In the combustor, the energy balance can be written as:

$$\dot{Q}_C + \dot{Q}_{cmb,H_2} + \dot{Q}_{cmb,O_2} + \dot{Q}_{icw} = \dot{Q}_{cmb,pw} + \dot{Q}_{evp,g,out} + \dot{Q}_{clw} \tag{63}$$

where, Q_{cmb,H_2} is heat carried into combustor by hydrogen. Q_{cmb,O_2} is heat carried into combustor by oxidizer. $Q_{cmb,pw}$ is heat absorbed by the product of H_2O. $Q_{evp,g,out}$ is heat absorbed by superheated vapor from evaporator. $\dot{Q}_{clw}$ is heat absorbed by cooling water from pump.

The mass balance can be written as:

$$\dot{m}_{cmb} = \dot{m}_{icw} + \dot{m}_{cmb,pw} + \dot{m}_{evp} + \dot{m}_{clw} \tag{64}$$

where, $\dot{m}_{cmb}$ is steam flow at combustor outlet. $\dot{m}_{cmb,pw}$ is flow of product H_2O . $\dot{m}_{clw}$ is flow of cooling water.

According to the chemical equation:

$$\dot{m}_{O_2} = \frac{8\dot{m}_{rdu,rw}}{9} \tag{65}$$

So,

$$\dot{m}_{cmb,pw} = \dot{m}_{rdu,rw} \tag{66}$$

Exothermic power of chemical reaction can be written as:

$$\dot{Q}_C = \dot{m}_{rdu,rw} Q_C \tag{67}$$

4.3. Turbine

Mass balance for the turbine can be written as:

$$\dot{m}_{nz} - \dot{m}_{cnd,g,in} = V_{trb} \frac{d\rho_{cnd,g,in}}{dt} \tag{68}$$

where, V_{trb} is capacity of turbine hall. $\dot{m}_{cnd,g,in}$ and $\rho_{cnd,g,in}$ are flow and density of vapor at the inlet of condenser. $\dot{m}_{nz}$ is nozzle flow, which can be described as:

$$\dot{m}_{nz} = \dot{m}_{nz,s} \frac{p_{cmb}}{p_{cmb,s}} \sqrt{\frac{T_{cmb,s}}{T_{cmb}}} \tag{69}$$

And,

$$\frac{d\rho_{cnd,g,in}}{dt} = \frac{d\rho_{cnd,g,in}}{dh_{cnd,g,in}} \frac{dh_{cnd,g,in}}{dt} \tag{70}$$

Here, $h_{cnd,g,in}$ is specific enthalpy of vapor at the inlet of condenser.

The energy balance can be written as:

$$\begin{aligned} \dot{m}_{nz} h_{trb,out} - \dot{m}_{cnd,g,in} h_{cnd,g,in} &= V_{trb} \frac{d(\rho_{cnd,g,in} u_{cnd,g,in})}{dt} \\ &= V_{trb} \frac{d}{dt} \left[\rho_{cnd,g,in} \left(h_{cnd,g,in} - \frac{p_d}{\rho_{cnd,g,in}} \right) \right] \\ &= V_{trb} \frac{d}{dt} (\rho_{cnd,g,in} h_{cnd,g,in} - p_d) \\ &= V_{trb} \left(h_{cnd,g,in} \frac{d\rho_{cnd,g,in}}{dt} + \rho_{cnd,g,in} \frac{dh_{cnd,g,in}}{dt} \right) \end{aligned} \tag{71}$$

where, p_d is pressure at the outlet of condenser.

Enthalpy drop of nozzle is:

$$h_{nz} = h_{cmb} - h_{nz,out} \tag{72}$$

Specific enthalpy of exhaust gas at the outlet of turbine hall is:

$$h_{trb,out} = h_{cmb} - h_{nz}\eta_i \tag{73}$$

Inserting Eqs. (63) and (64) into Eq. (62) yields:

$$V_{trb}\rho_{cnd,g,in} \frac{dh_{cnd,g,in}}{dt} = \dot{m}_{nz}(h_{trb,out} - h_{cnd,g,in}) \tag{74}$$

So, $\frac{dh_{cnd,g,in}}{dt}$ and $\dot{m}_{cnd,g,in}$ can be calculated from Eqs. (70), (71) and (74).

According to isentropic flow theory, theoretical velocity at the outlet of nozzle can be written as:

$$v_{nz} = \sqrt{\frac{2kR_g T_{cmb}}{k-1} \left(1 - B_{nz}^{\frac{k-1}{k}}\right)} \tag{75}$$

Relative velocity at the inlet of turbine hall is:

$$w_{trb,in} = \sqrt{(v_{nz}\sin\alpha_{nz})^2 + (v_{nz}\cos\alpha_{nz} - u_{trb})^2} \tag{76}$$

Wheel power of turbine can be written as:

$$P_u = (w_{trb,in}\cos\beta_{trb,in} + w_{trb,out}\cos\beta_{trb,out})u_{trb} \tag{77}$$

Inlet blade angle of turbine can be calculated:

$$\cos\beta_{trb,in} = \frac{v_{nz}\cos\alpha_{nz} - u_{trb}}{w_{trb,in}} \tag{78}$$

Wheel efficiency η_u of turbine can be calculated:

$$\eta_u = \frac{P_u}{0.5 v_{nz}^2} \tag{79}$$

Internal efficiency η_i of turbine can be calculated as [31]:

$$\eta_i = \eta_u(1 - 0.08\eta_u)\left(1 - 0.5e^{\frac{\varepsilon}{0.1}}\right) \tag{80}$$

5. Model comparative analysis

For comparison, both simulations with modified model and with previous model are carried out with MATLAB using discretized method. General equations of the previous model in literatures [12–20] is Eqs. (1) and (2).

And, the following values have been used in the numerical simulation:

(1) Initial temperature inside of reactor is 1000 K.
(2) Diameter of turbine is 0.08 m; Volume of turbine hall is 0.003 m^3; Power loss coefficient is 0.6; Nozzle efficiency is 0.94; Initial turbine speed is 100,000 rpm, and output power is 90 kW.
(3) Volume of combustor is 0.001 m^3; Initial temperature inside of combustor is 900 K.

(4) Inner diameter of evaporator pipe is 0.034 m, and for condenser is 0.010 m.
(5) Mass of reagent water in the reactor $m_{rdu,rw} = 0.5m_1$.

5.1. Model comparison

The reagent water flow rate which is an input variable in reactor was perturbed with the other input variables held constant. Two important time constants are identified from the simulation in this section:

- At time 2 s, reagent water flow rate was step decrease to 95% of primary rate.
- At time 15 s, reagent water flow rate was step increase to 105% of primary rate.

Both simulations with previous model in literatures [12–20] and with modified model in this paper were applied. The simulation results are presented in the form of a series of curves representing the transient response of the process variables.

And, in order to facilitate comparative analysis, some of the simulation results have been normalized. Transient responses of the region lengths (i.e., subcooled, two-phase and superheated) in evaporator and condenser are given in Figs. 5 and 6. Fig. 7 shows the transient response of the system temperature. And, in each case, the simulation results with previous model and with modified model are presented separately.

According to the figures, important phenomena to include in the simulation results are: when using the previous model, each process variable displays an initial reverse oscillation with a subsequent asymptotic behavior, especially the length of two-phase region and superheated region. The oscillation is known as *Chattering*. Probably, these oscillations in the previous model results are generated due to lose sight of the relative velocities between the fluid and boundaries. Results obtained from the modified model are much realistic appraisal of the situation.

5.2. Dynamic simulation and discussion

For control system design, dynamic simulations have been carried out. The results show the system transient responses for up to 70% decrease and increase in mass flow rate of reagent water with the other input variables held constant. For more realistic, mass flow rate of reagent water was perturbed in cosine curve. And the simulation results are shown in the following Figs. 8–13.

(1) Decreased reagent water mass flow decreases the exothermic heat of chemic reaction in the reactor, as well as in combustor. Mass flows of water outlet of nozzle, cooling water (Fig. 8) decrease. And output power of turbine (Fig. 9) is also decreases due to the reduction of pressure in combustor. A similar phenomenon exists for a cosine increase in reagent water flow rate.

(2) With the decreased reagent water mass flow rate, a special phenomenon exits for the temperature of steam leaving the evaporator (Fig. 10), which increases steadily to a new value, after a small initial dip.

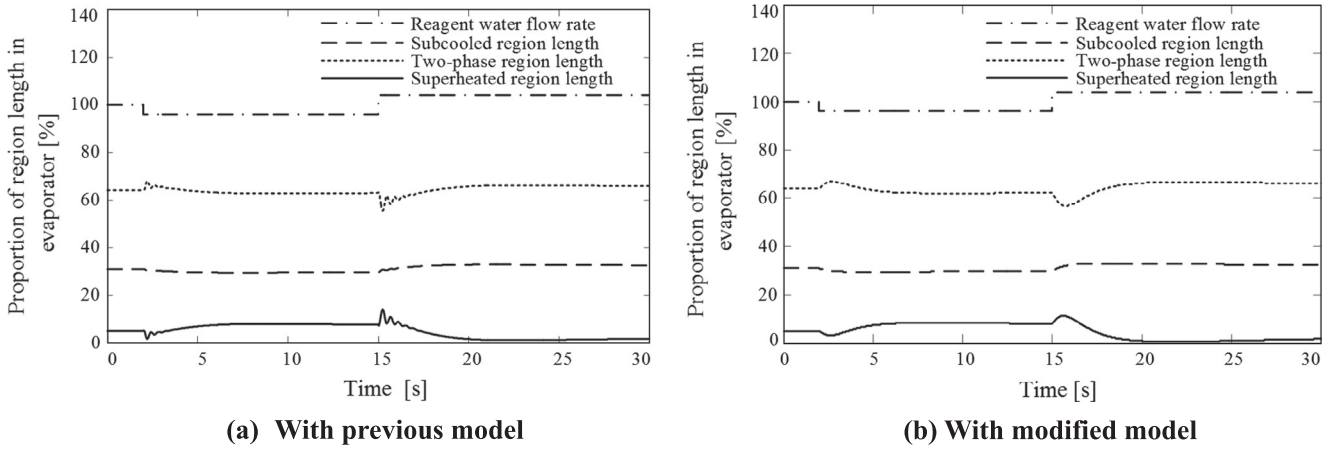

Fig. 5. Transient response of region length in evaporator.

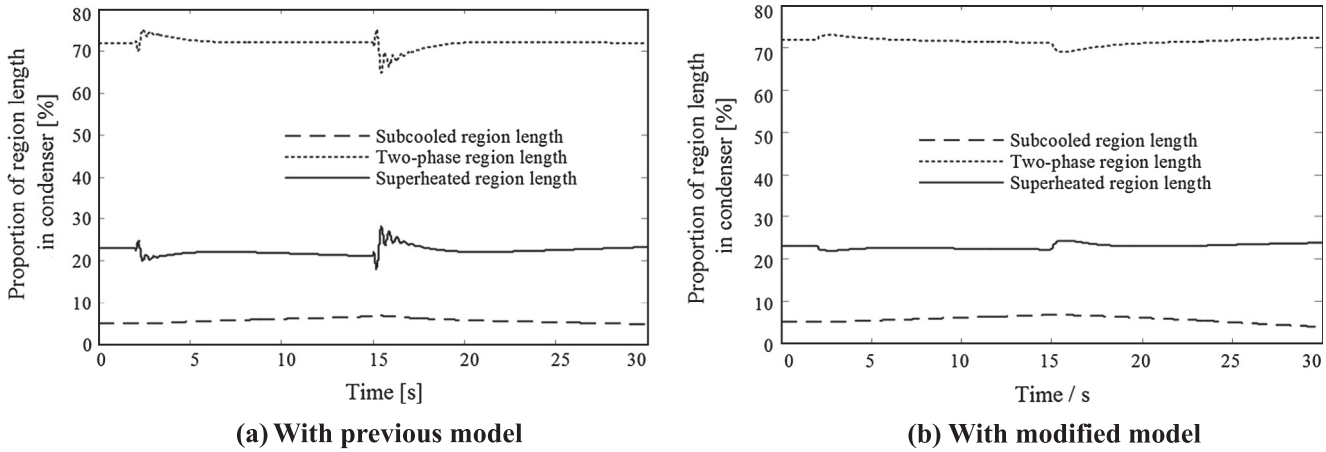

Fig. 6. Transient response of region length in condenser.

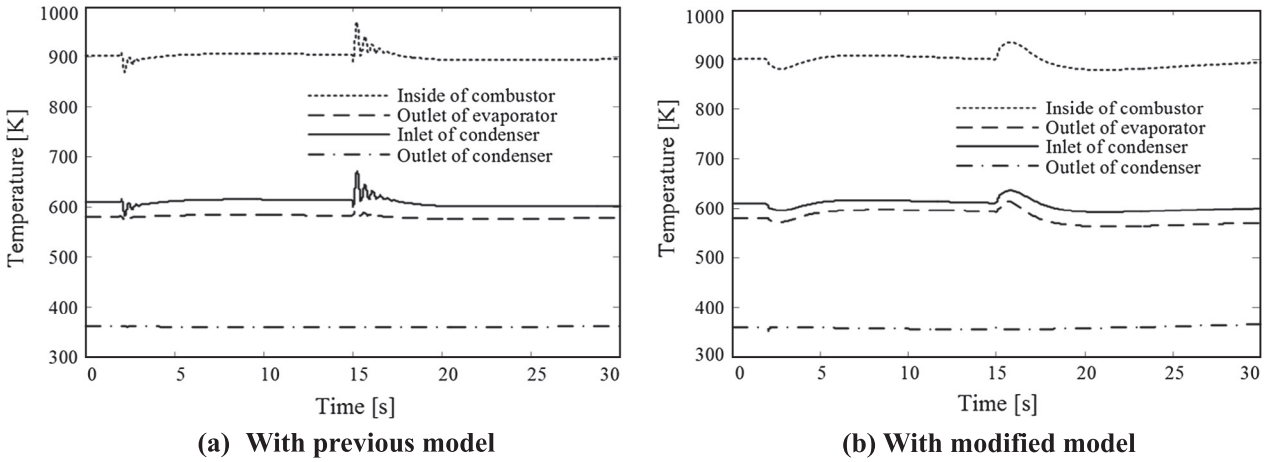

Fig. 7. Transient response of system temperature.

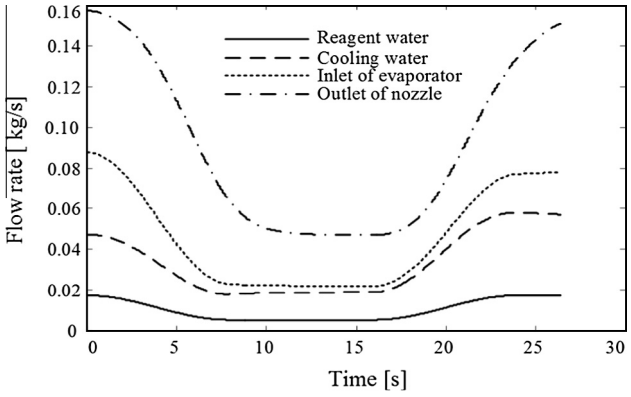

Fig. 8. Dynamic process of water flow rate.

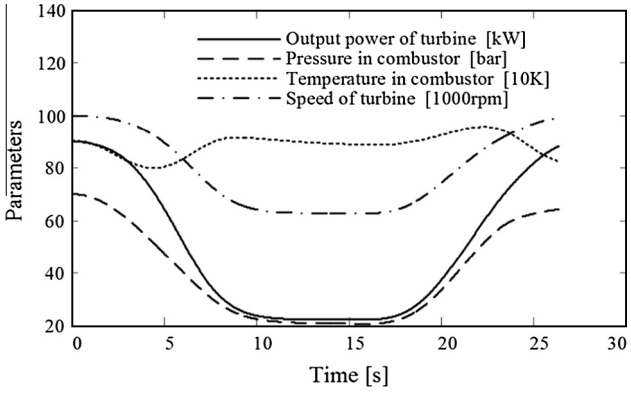

Fig. 9. Dynamic process of turbine system.

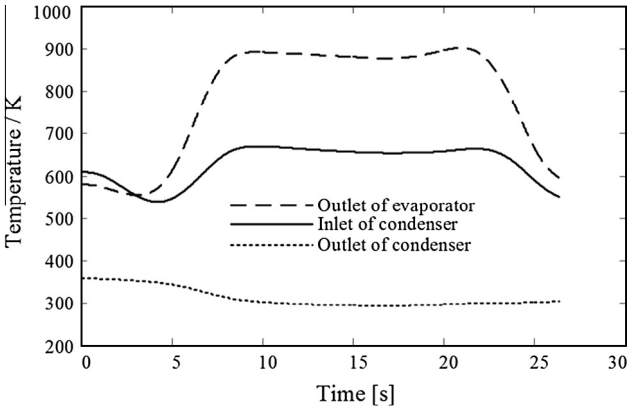

Fig. 10. Dynamic process of temperature.

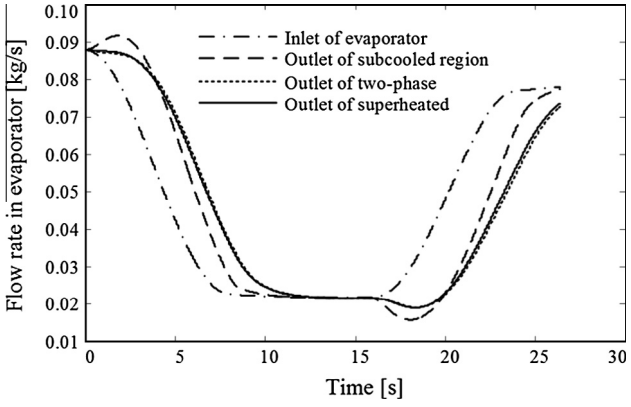

Fig. 11. Flow rate in evaporator.

This is because, within a short time in the beginning of perturb, length of subcooled region will reduce (Fig. 12) due to the mass flow rate drop at the inlet of evaporator (Fig. 8). But, according to the mass balance equation of subcooled region Eq. (21), mass flow of outlet of subcooled region in evaporator (Fig. 11) would increase. In this case, coupling effects of temperature reduction in reactor and initial reverse of outlet mass flow of subcooled region in evaporator, the length of two-phase region (Fig. 12) would initially rise. So, for a given evaporator length, the length of superheated region (Fig. 12) would initially dip. And the outlet temperature of evaporator (Fig. 10) would also be a corresponding change.

With the continued decrease of reagent water mass flow, outlet flow rate of each phase region (Fig. 11) would decrease continuously. Lengths of subcooled region and two-phase (Fig. 12) reduce due to the mass flow drop. Also, for a given evaporator length, the length of superheated region (Fig. 12), after a small initial dip, would increase steadily to a new value, which causes temperature rising (Fig. 10) of steam leaving the evaporator.

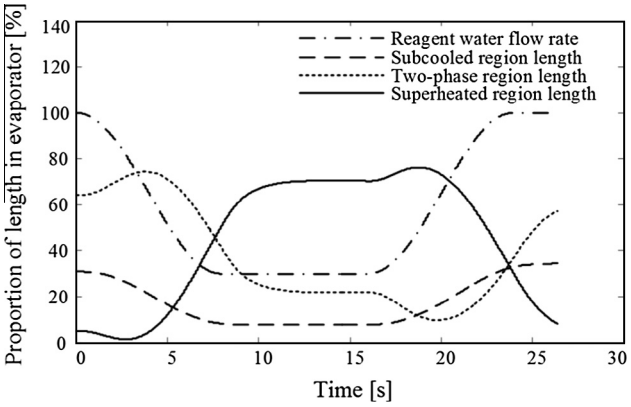

Fig. 12. Region length in evaporator.

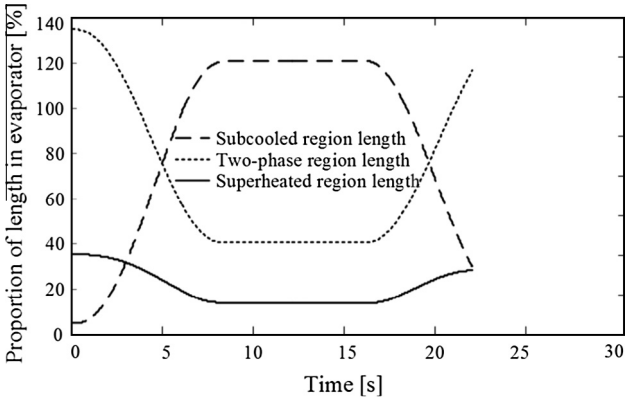

Fig. 13. Region length in condenser.

(3) Analogously, the special phenomenon exits for the temperatures in combustor (Fig. 9) and inlet of condenser (Fig. 10), which are also initially dip and then approach the new value as there is no increase in reagent water flow rate to sustain the rise. Within a short time in the beginning of perturb, decrease of temperature in combustor (Fig. 9) is caused by the coupling effects of exothermic heat decrease in combustor and temperature decrease of steam leaving the evaporator (Fig. 10). Continuing of reagent water mass flow rate decrease, temperature in combustor approaches the original value (Fig. 9) due to the continuous improvement of temperature of steam leaving the evaporator (Fig. 10), and the continued reduction of cooling water flow (Fig. 8). And, temperature at inlet of condenser (Fig. 10) shows a similar variation, which is directly affected by the temperature in combustor.

(4) Due to the reduction of water mass flow in the system, lengths of superheated region and two-phase region in the condenser decrease, but subcooled region increases (Fig. 13).

6. Conclusions

In this paper, the general governing equations of the previous MB model for describing the dynamics of a two-phase flow heat exchanger (evaporator or condenser) were analyzed, pointing out the defect of ignoring the relative velocities between boundaries and fluid. And when using the model, each process variable displays an initial reverse oscillation with a subsequent asymptotic behavior.

For the existing defect, a modified MB model has been presented, which derived from physical principles of mass and energy conservation. One of the main features of this model is an explicit inclusion of relative velocities between fluid and boundaries. And modified model is then implemented in an underwater HYDROX system to predict cyclic performance. The simulation results which do not appear *Chattering*, compare favorably to those obtained with the previous model. The system transients derived from this model can be used as an element in designing of appropriate control systems.

Acknowledgements

The project is supported by the National Natural Science Foundation of China (NSFC) (Grant No. 51409215). The authors would like to thank them for the sponsorship.

Reference

[1] S. Bendapudi, J.E. Braun, A Review of Literature on Dynamic Models of Vapor Compression Equipment. Technical Report HL2002-8. Ray W. Herrick Laboratories, Purdue University, 2002.
[2] E.W. Grald, J.W. MacArthur, A moving-boundary formulation for modeling time-dependent two-phase flows, Int. J. Heat Fluid Flow 13 (3) (1992) 266–272.
[3] T. Cheng, H.H. Asada, Nonlinear observer design for a varying-order switched system with application to heat exchangers, in: Proceedings of the ACC. IEEE, Minneapolis, MN, USA, 2006, pp. 2898–2903.
[4] J. Adams, D.R. Clark, J.R. Louis, J.P. Spanbauer, Mathematical modeling of once-through boiler dynamics, IEEE Trans. Power Apparatus Syst. 84 (2) (1965) 146–156.
[5] A. Ray, H. Bowman, A nonlinear dynamic model of a once-through subcritical steam generator, J. Dyn. Syst., Meas., Control 98 (3) (1976) 332–339.
[6] A. Ray, Dynamic modelling of once-through subcritical steam generator for solar applications, Appl. Math. Model. 4 (6) (1980) 417–423.
[7] A. Ray, Nonlinear dynamic model of a solar steam generator, Solar Energy 26 (2) (1981) 297–306.
[8] M. Dhar, W. Soedel, Transient analysis of a vapor compression refrigeration system, in: Proceedings of the XVth International Congress of Refrigeration, Venice, Italy, 1979.
[9] T.L. Mckinley, A.G. Alleyne, An advanced nonlinear switched heat exchanger model for vapor compression cycles using the moving-boundary method, Int. J. Refrig. 31 (7) (2008) 1253–1264.
[10] F. Mancini, Energy efficiency improvements of household heat pump systems [Ph.D. Thesis]. Padova, Italy: University of Padova, 2011.
[11] B.P. Rasmussen, Dynamic modeling for vapor compression systems – part I: literature review, HVAC&R Res. 18 (5) (2012) 934–955.
[12] J. Bonilla, L.J. Yebra, S. Dormido, F.E. Cellier, Object-oriented modeling of switching moving boundary models for two-phase flow evaporators, in: Proceedings MATHMOD 2012–7th Vienna International Conference on Mathematical Modelling, 2012.
[13] J. Bonilla, L.J. Yebra, S. Dormido, F.E. Cellier, Object-oriented library of switching moving boundary models for two-phase flow evaporators and condensers, in: 9th International Modelica Conference, Munich, Germany, 2012, pp. 71–80.
[14] J. Bonilla, S. Dormido, F.E. Cellier, Switching moving boundary models for two-phase flow evaporators and condensers, Commun. Nonlinear Sci. Numer. Simul. 20 (2015) 743–768.
[15] X.D. He, S. Liu, H.H. Asada, Modeling of vapor compression cycles for advanced controls in HVAC systems, in: Proceedings of the American Control Conference, Seattle, Washington, June 1995, pp. 3664–3668.
[16] X.D. He, S. Liu, H.H. Asada, H. Itoh, Multivariable control of vapor compression systems, HVAC&R Res. 4 (3) (1998) 205–230.
[17] D. Wei, X. Lu, Z. Lu, J. Gu, Dynamic modeling and simulation of an organic rankine cycle (ORC) system for waste heat recovery, Appl. Therm. Eng. 28 (10) (2008) 1216–1224.
[18] J.M. Jensen, Dynamic modeling of thermo-fluid systems [Ph.D. Thesis]. Denmark: Technical University of Denmark, 2003.
[19] J.M. Jensen, H. Tummescheit, Moving boundary models for dynamic simulations of two-phase flows, in: 2nd International Modelica Conference, Oberpfaffenhofen, Germany, 2002.
[20] L.J. Yebra, M. Berenguel, S. Dormido, Extended moving-boundary models for two-phase flows, in: 16th IFAC World Congress, Praha, 2005.
[21] B. Li, A.G. Alleyne, A dynamic model of a vapor compression cycle with shut-down and start-up operations, Int. J. Refrig. 33 (5) (2010) 538–552.
[22] M. Gräber, N.C. Strupp, W. Tegethoff, Moving boundary heat exchanger model and validation procedure, in: 8th EUROSIM Congress on Modelling and Simulation, Prague, Czech Republic, 2010.
[23] L. Cecchinato, F. Mancini, An intrinsically mass conservative switched evaporator model adopting the moving-boundary method, Int. J. Refrig. 35 (2) (2012) 349–364.
[24] J.I. Zapata, J. Pye, K. Lovegrove, A transient model for the heat exchange in a solar thermal once through cavity receiver, Solar Energy 93 (2013) 280–293.

[25] C. Tian, C. Dou, X. Yang, X. Li, Instability of automotive air conditioning system with a variable displacement compressor. Part 2. Numerical simulation, Int. J. Refrig. 28 (7) (2005) 1111–1123.
[26] C. Tian, X. Li, Transient behavior evaluation of an automotive air conditioning system with a variable displacement compressor, Appl. Therm. Eng. 25 (13) (2005) 1922–1948.
[27] V. Gnielinski, New equations for heat and mass-transfer in turbulent pipe and channel flow, Int. Chem. Eng. 16 (2) (1976) 359–368.
[28] G.K. Filonenko, Hydraulic resistance in pipes (in Russian), Teploenergetika 1 (4) (1954) 40–44.
[29] S.G. Kandlikar, A general correlation for saturated two-phase flow boiling heat transfer inside horizontal and vertical tubes, J. Heat Transfer 112 (1990) 219–228.
[30] A.J. Ghajar, L.M. Tam, Heat transfer measurements and correlations in the transition region for a circular tube with three different inlet configurations, Exp. Therm. Fluid Sci. 8 (1) (1994) 79–90.
[31] D.H. Kiely, J.T. Moore, Hydrocarbon fueled UUV power systems, in: Proceedings of the Symposium on Autonomous Underwater Vehicle Technology, San Antonio TX, June 2002, pp. 121–128.